SYNTHETIC BIOLOGY

Mirror-image T7 transcription of chirally inverted ribosomal and functional RNAs

Yuan Xu[1,2,3] and Ting F. Zhu[2,3]*

To synthesize a chirally inverted ribosome with the goal of building mirror-image biology systems requires the preparation of kilobase-long mirror-image ribosomal RNAs that make up the structural and catalytic core and about two-thirds of the molecular mass of the mirror-image ribosome. Here, we chemically synthesized a 100-kilodalton mirror-image T7 RNA polymerase, which enabled efficient and faithful transcription of the full-length mirror-image 5*S*, 16*S*, and 23*S* ribosomal RNAs from enzymatically assembled long mirror-image genes. We further exploited the versatile mirror-image T7 transcription system for practical applications such as biostable mirror-image riboswitch sensor, long-term storage of unprotected kilobase-long L-RNA in water, and L-ribozyme–catalyzed L-RNA polymerization to serve as a model system for basic RNA research.

More than 160 years after Louis Pasteur's discovery of molecular chirality and proposal of a chirally inverted form of life (*1*), mirror-image life has not been discovered in nature. The laboratory realization of in vitro mirror-image biology systems with D-amino acids and L-nucleic acids as the building blocks (as opposed to the natural-chirality L-amino acids and D-nucleic acids) presents unique opportunities but remains challenging. An important part of this effort is establishing a mirror-image version of the central dogma of molecular biology (*2*, *3*). After mirror-image DNA replication, transcription, and reverse transcription (*2*, *4*–*8*), the next step is to realize mirror-image translation (Fig. 1A) (*3*, *9*, *10*). This requires high-quality long L-RNAs such as the kilobase-long mirror-image ribosomal RNAs (rRNAs), which make up the structural and catalytic core of the >2-MDa mirror-image ribosome.

The chemical synthesis of high-quality long L-RNAs remains difficult because traditional phosphoramidate chemistry only allows efficient RNA synthesis of up to 60 to 70 nucleotides (nt) (*11*). One way to overcome this limitation is through enzymatic transcription by mirror-image polymerases. We previously used a Y12S mutant of the mirror-image *Sulfolobus solfataricus* P2 DNA polymerase IV (D-Dpo4-5m-Y12S) to transcribe a 120-nt mirror-image *Escherichia coli* (*E. coli*) 5*S* rRNA (*7*). Additionally, cross-chiral ribozymes have been developed to polymerize L-RNAs (*12*, *13*). However, both systems suffer from low efficiency and fidelity, and require single-stranded L-DNA or L-RNA templates, which are difficult to prepare and remove from the polymerized L-RNAs.

[1]School of Life Sciences, Tsinghua-Peking Center for Life Sciences, Beijing Frontier Research Center for Biological Structure, Tsinghua University, Beijing, China. [2]School of Life Sciences, Research Center for Industries of the Future, Westlake University, Hangzhou, Zhejiang, China. [3]Westlake Laboratory of Life Sciences and Biomedicine, Hangzhou, Zhejiang, China.
*Corresponding author. Email: tzhu@westlake.edu.cn

An alternative is to synthesize a mirror-image version of the bacteriophage T7 RNA polymerase, which is a widely used workhorse enzyme for both in vitro and in vivo transcription in the laboratory because of its excellent efficiency, fidelity, and promoter specificity (*14*). The T7 RNA polymerase uses double-stranded DNA templates for transcription, the mirror-image version of which can be readily assembled by mirror-image polymerase chain reaction (PCR) (*4*–*6*, *8*). However, the full-length T7 RNA polymerase contains 883 amino acids, beyond the general size limit for chemical protein synthesis that combines solid-phase peptide synthesis (SPPS) (*15*) with native chemical ligation (NCL) (*16*), enabling the synthesis of various mirror-image enzymes (*2*, *5*, *6*, *17*–*21*) typically smaller than ~400 amino acids, or ~45 kDa. Recently, we applied split-protein design and systematic isoleucine substitution to facilitate the total chemical synthesis of a 90-kDa high-fidelity mirror-image *Pfu* DNA polymerase, which enabled the accurate assembly of a 1.5-kb mirror-image 16*S* rRNA gene (*8*). Although we also developed a mutant *Pfu* DNA polymerase for transcribing RNA, the suboptimal transcription efficiency and difficulty in preparing long single-stranded L-DNA templates will likely make this approach impractical (*8*). Here, we set out to synthesize a 100-kDa mirror-image T7 RNA polymerase using split-protein design and systematic isoleucine substitution and test its ability to efficiently and faithfully transcribe high-quality long L-RNAs such as the mirror-image 5*S*, 16*S*, and 23*S* rRNAs and various functional L-RNAs.

Results

Design and synthesis of a 100-kDa mirror-image T7 RNA polymerase

Split-protein design divides a large (natural-chirality or mirror-image) protein into two or more smaller split-protein fragments that can co-fold in vitro into a functionally intact enzyme (*8*). Many enzymes have naturally occurring or engineered split versions, including the T7 RNA polymerase (*22*, *23*). However, some of the previously reported split sites alter its transcription efficiency (*22*) or are near the N or C terminus of the polymerase (*22*, *23*), resulting in split-protein fragments larger than 400 amino acids, which are difficult to chemically synthesize. We designed a double-split version of the T7 RNA polymerase with a previously reported split site between N601 and T602 (*23*) and a newly discovered split site between K363 and P364 in a solvent-exposed loop, dividing the 883–amino acid polymerase into three split-protein fragments: the 363–amino acid N fragment, the 238–amino acid M fragment, and the 282–amino acid C fragment (Fig. 1B). Additionally, we substituted 14 of the 51 isoleucines in the polymerase with valine, leucine, and methionine (fig. S1 and table S1) to facilitate the chemical protein synthesis and to reduce the D-amino acid costs (*8*). We next biochemically validated the design by comparing the transcription efficiencies of the recombinant wild-type (WT) and recombinant double-split mutant (containing 14 isoleucine substitutions) T7 RNA polymerases at various enzyme concentrations with a double-stranded D-DNA template, and observed similar transcription efficiencies between them (fig. S2).

We then performed total chemical synthesis of the double-split mutant version of both the natural-chirality and mirror-image T7 RNA polymerases (hereafter referred to as the synthetic natural-chirality and synthetic mirror-image T7 RNA polymerases, respectively). The N, M, and C fragments of the natural-chirality and mirror-image polymerases were each divided into five to eight peptide segments ranging from 20 to 76 amino acids in length (figs. S3 to S6 and table S2). All of the peptide segments were prepared by 9-fluorenylmethoxycarbonyl (Fmoc)-SPPS, purified by reversed-phase high-performance liquid chromatography (RP-HPLC), and assembled by hydrazide-based NCL (*24*), followed by metal-free radical-based desulfurization (*25*) to convert unprotected cysteine to alanine (*26*). After the synthesis, ligation, purification, and lyophilization (figs. S7 to S55), the N, M, and C fragments of the natural-chirality and mirror-image polymerases were obtained at milligram scales with the expected molecular masses of 41.4, 26.8, and 31.5 kDa, respectively, totaling ~100 kDa (table S2). Both the synthetic natural-chirality and synthetic mirror-image T7 RNA polymerases were folded in vitro by dialysis, as validated by 8-anilino-1-naphthalene sulfonate (ANS) fluorescence (fig. S56), and analyzed by SDS-polyacrylamide gel electrophoresis (SDS-PAGE) (Fig. 1C).

Mirror-image T7 transcription of short L-RNAs

We tested the transcription activity of the synthetic mirror-image T7 RNA polymerase with a double-stranded L-DNA template coding for the *Thermus thermophilus* (*T. thermophilus*)

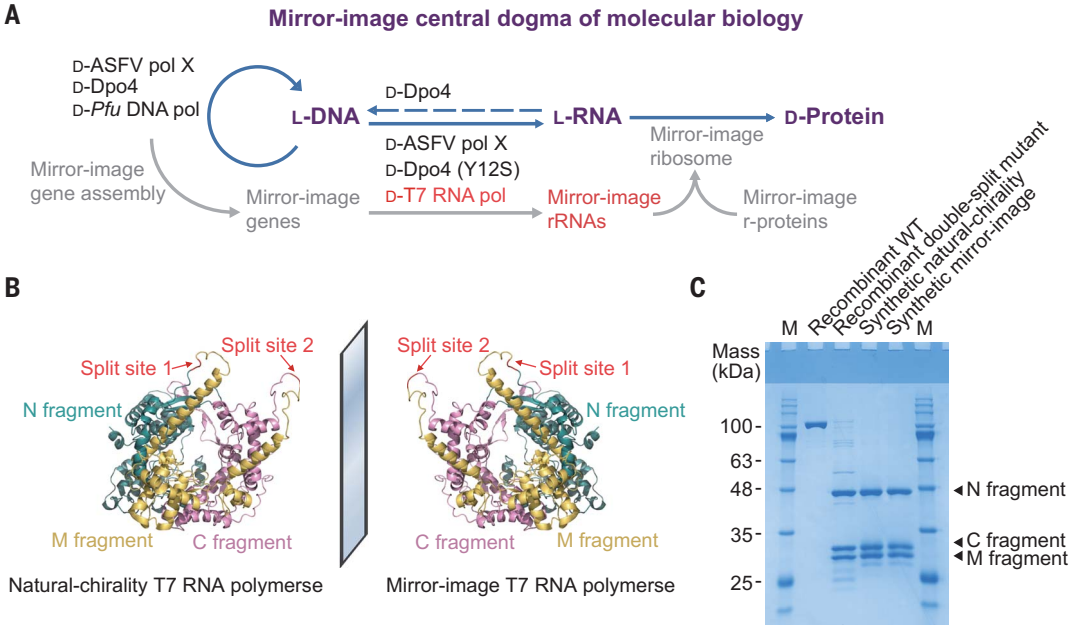

Fig. 1. Synthetic natural-chirality and synthetic mirror-image T7 RNA polymerases. (**A**) Mirror-image version of the central dogma of molecular biology, including mirror-image DNA replication, transcription, reversetranscription, and translation (blue arrows), and the role of the synthetic mirror-image T7 RNA polymerase in transcribing the mirror-image rRNAs (shown in red) to be assembled with the mirror-image ribosomal proteins (r-proteins) into a mirror-image ribosome. (**B**) Structure of the WT T7 RNA polymerase (Protein Data Bank ID: 1CEZ) in natural-chirality and mirror-image forms. The N fragment is shown in green, the M fragment in yellow, and the C fragment in pink, with the amino acids at the two split sites (K363 and P364, N601 and T602) shown in red. (**C**) Recombinant WT, recombinant double-split mutant, synthetic natural-chirality, and synthetic mirror-image T7 RNA polymerases analyzed by SDS-PAGE and stained by Coomassie brilliant blue. M, protein marker.

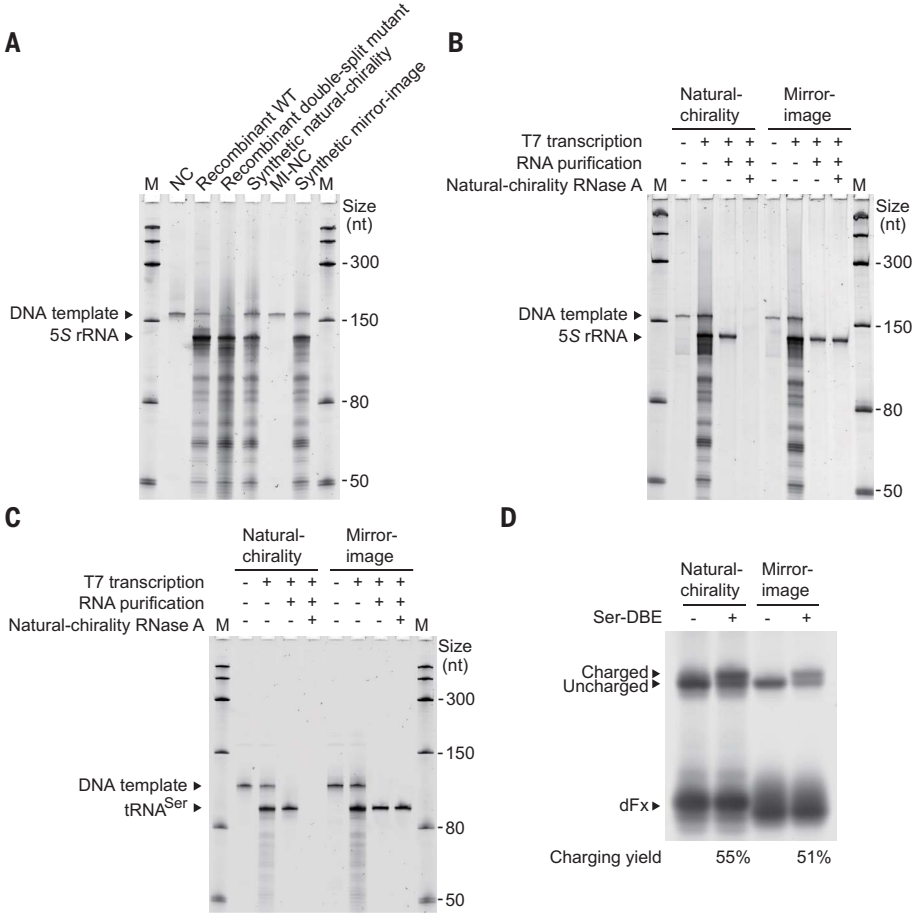

Fig. 2. Mirror-image T7 transcription of short L-RNAs. (**A**) Transcription of the natural-chirality and mirror-image 122-nt 5*S* rRNAs from the double-stranded D- or L-DNA template by the recombinant WT, recombinant double-split mutant, synthetic natural-chirality, and synthetic mirror-image T7 RNA polymerases, respectively, analyzed by denaturing PAGE and stained by SYBR green II. NC and MI-NC, negative controls without natural-chirality or mirror-image T7 RNA polymerase, respectively; M, Low Range ssRNA ladder. (**B** and **C**) Transcription of the natural-chirality and mirror-image 122-nt 5*S* rRNAs (B) and 90-nt tRNAs^{Ser} (C) from the double-stranded D- or L-DNA template by the synthetic natural-chirality and synthetic mirror-image T7 RNA polymerases, respectively, purified by denaturing PAGE, treated by natural-chirality RNase A, analyzed by denaturing PAGE, and stained by SYBR green II. M, Low Range ssRNA ladder. (**D**) Natural-chirality and mirror-image dFx charging of L- or D-serine onto the natural-chirality and mirror-image tRNAs^{Ser} with L- or D-Ser-DBE, respectively, analyzed by acid PAGE and stained by SYBR green II.

5*S* rRNA (tables S5 to S7) assembled by mirror-image PCR (*5*), and found that it was capable of transcribing the full-length 122-nt mirror-image 5*S* rRNA (Fig. 2A) despite having lower efficiency than the recombinant WT, recombinant double-split mutant, and synthetic natural-chirality polymerases (fig. S57). The gel-purified 122-nt mirror-image 5*S* rRNA was resistant to natural-chirality ribonuclease A (RNase A) digestion (Fig. 2B). Because of the lack of high-fidelity mirror-image reverse transcriptase and Sanger sequencing tools, we were

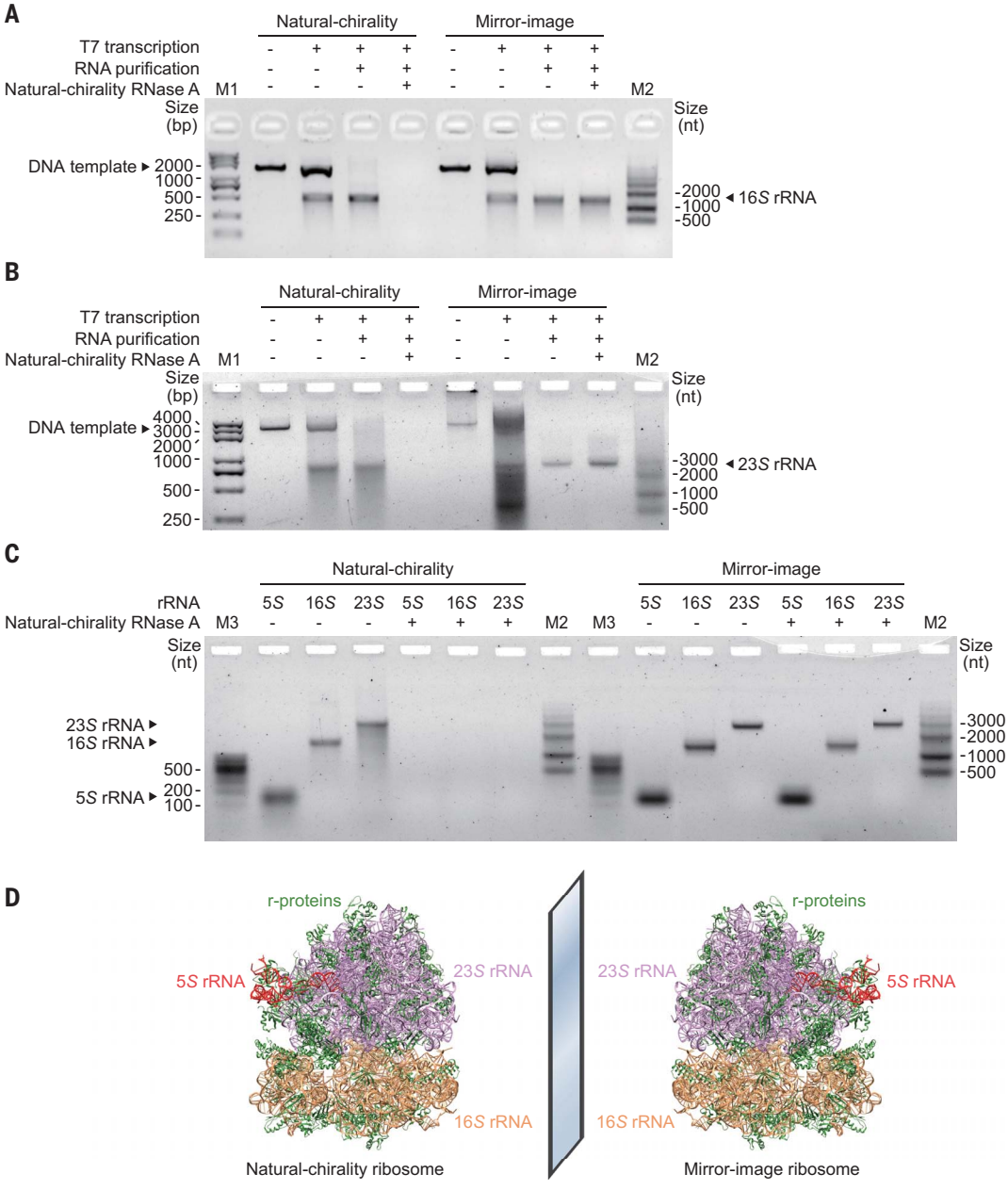

Fig. 3. Mirror-image T7 transcription and purification of kilobase-long mirror-image rRNAs. (**A** and **B**) Transcription of the natural-chirality and mirror-image 1.5-kb 16*S* (A) and 2.9-kb 23*S* (B) rRNAs from the double-stranded D- or L-DNA template by the synthetic natural-chirality and synthetic mirror-image T7 RNA polymerases, respectively, purified by low-melting-point agarose gel electrophoresis and β-agarase I digestion, treated by natural-chirality RNase A, analyzed by agarose gel electrophoresis, and stained by ExRed. M1, Trans2K Plus DNA marker; M2, RNA marker RL6,000. (**C**) Gel-purified natural-chirality and mirror-image 122-nt 5*S*, 1.5-kb 16*S*, and 2.9-kb 23*S* rRNAs treated by natural-chirality RNase A, analyzed by agarose gel electrophoresis, and stained by ExRed. M2, RNA marker RL6,000; M3, RNA marker RL1,000. (**D**) Structure of the *T. thermophilus* ribosome (Protein Data Bank ID: 4V4P) in natural-chirality and mirror-image forms, showing the 5S rRNA in red, 16S rRNA in gold, 23S rRNA in pink, and r-proteins in green.

unable to evaluate the transcription fidelity of the synthetic mirror-image T7 RNA polymerase directly, and thus we examined the transcription fidelity of the synthetic natural-chirality T7 RNA polymerase as an estimate for the mirror-image version. We reverse-transcribed the DNase-treated transcription product of the synthetic natural-chirality T7 RNA polymerase by a high-fidelity reverse transcriptase, followed by high-fidelity PCR and Sanger sequencing (fig. S58). We measured the error rate of the synthetic natural-chirality T7 RNA polymerase on the order of 10^{-4}, consistent with those of the recombinant WT and recombinant double-split mutant polymerases, as well as the WT polymerase reported in previous studies (table S3) (*27*).

Toward realizing mirror-image translation, we previously used a mirror-image version of the 46-nt dinitro-flexizyme (dFx) (*28*) to charge three D-amino acids (D-lysine, D-alanine, and D-phenylalanine) and the achiral glycine onto the corresponding mirror-image transfer RNAs (tRNAs) transcribed by D-Dpo4-5m-Y12S (*10*). However, D-Dpo4-5m-Y12S was unable to transcribe certain mirror-image tRNA sequences, such as the 90-nt mirror-image serine tRNA ($tRNA^{Ser}$) (fig. S59), likely because of the length and extensive secondary structure of the single-stranded L-DNA template. We addressed this issue by mirror-image T7 transcription with a double-stranded L-DNA template coding for $tRNA^{Ser}$ (tables S5 to S7) assembled by mirror-image PCR (*5*). We found that the transcription efficiency of the 90-nt mirror-image $tRNA^{Ser}$ by the synthetic mirror-image T7 RNA polymerase was substantially higher than that by D-Dpo4-5m-Y12S (fig. S59). The gel-purified 90-nt mirror-image $tRNA^{Ser}$ was resistant to natural-chirality RNase A digestion (Fig. 2C). Furthermore, we charged D-serine onto the mirror-image $tRNA^{Ser}$ using the mirror-image dFx and D-Ser-3,5-dinitrobenzyl ester (Ser-DBE), with a charging yield similar to that of the natural-chirality version (Fig. 2D).

Mirror-image T7 transcription and purification of kilobase-long mirror-image rRNAs

Encouraged by the results of the transcription and purification of short L-RNAs, we performed the mirror-image T7 transcription of the

kilobase-long mirror-image rRNAs. Using double-stranded L-DNA templates coding for the *T. thermophilus* 16*S* and 23*S* rRNAs (tables S5 to S7) assembled by mirror-image PCR (fig. S60) (*5*, *8*) and through further optimizing the transcription conditions, particularly for 23*S* rRNA (figs. S61 and S62), we transcribed the full-length mirror-image 1.5-kb 16*S* and 2.9-kb 23*S* rRNAs by the synthetic mirror-image T7 RNA polymerase (Fig. 3, A and B). Meanwhile, we also transcribed the natural-chirality rRNAs by the synthetic natural-chirality T7 RNA polymerase (Fig. 3, A and B).

Because a mirror-image DNase to digest L-DNA templates is unavailable, we purified the kilobase-long mirror-image 16*S* and 23*S* rRNAs from the double-stranded L-DNA templates by low-melting-point agarose gel electrophoresis and β-agarase I digestion (Fig. 3, A and B). The kilobase-long natural-chirality rRNAs and RNA markers were partially degraded despite our best effort to avoid natural-chirality RNase contamination and use of RNase inhibitor in conjunction, whereas the mirror-image 5*S*, 16*S*, and 23*S* rRNAs were stable (Fig. 3C), suggesting that the assembly of the mirror-image ribosome (Fig. 3D) could be more experimentally convenient to perform than the natural-chirality version because of the stability of the mirror-image rRNAs. We further evaluated the transcription fidelity of the synthetic natural-chirality T7 RNA polymerase (again, as an estimate for the mirror-image version) with double-stranded D-DNA templates coding for the 5*S*, 16*S*, and 23*S* rRNAs, and measured error rates on the order of 10^{-4}, consistent with that of the WT polymerase reported in previous studies (table S4) (*27*).

Mirror-image riboswitch sensor

Inspired by the broad utility of T7 transcription in the laboratory, we explored the practical applications of the mirror-image T7 transcription system through developing a 130-nt mirror-image riboswitch sensor by fusing a mirror-image guanine aptamer with a mirror-image Spinach aptamer according to the previously reported design (Fig. 4A) (*29*). Because both guanine and 3,5-difluoro-4-hydroxybenzylidene imidazolinone [DFHBI, the small-molecule fluorophore of the Spinach aptamer (*30*)] are achiral, the natural-chirality and mirror-image riboswitch sensors would be expected to exhibit identical binding characteristics. We transcribed the mirror-image riboswitch sensor by the synthetic mirror-image T7 RNA polymerase with a double-stranded L-DNA template (tables S5 to S7) assembled by mirror-image PCR (*5*). The gel-purified 130-nt mirror-image riboswitch sensor was resistant to natural-chirality RNase A digestion (Fig. 4B). We found that the natural-chirality and mirror-image riboswitch sensors exhibited nearly identical fluorescence intensities when incubated with

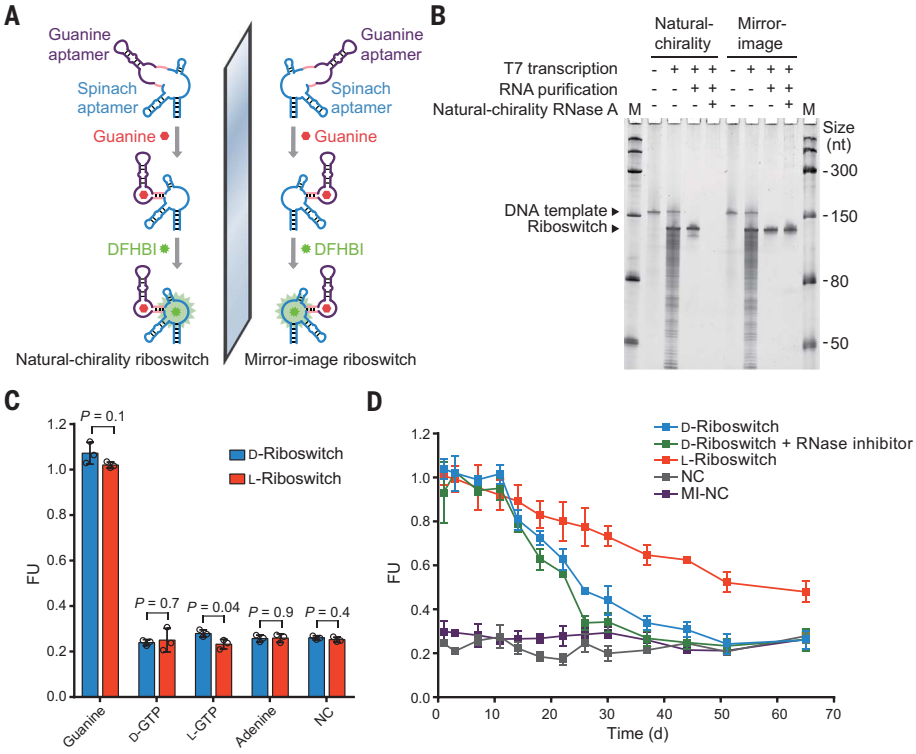

Fig. 4. Mirror-image riboswitch sensor. (**A**) Schematic overview of the natural-chirality and mirror-image riboswitch sensors by fusing a guanine aptamer (purple) with a Spinach aptamer (blue) through a "transducer" stem sequence (pink). (**B**) Transcription of the natural-chirality and mirror-image 130-nt riboswitch sensors from the double-stranded D- or L-DNA template by the synthetic natural-chirality and synthetic mirror-image T7 RNA polymerases, respectively, purified by denaturing PAGE, treated by natural-chirality RNase A, analyzed by denaturing PAGE, and stained by SYBR green II. M, Low Range ssRNA ladder. (**C**) Fluorescence intensities measured at 500 nm of the natural-chirality and mirror-image riboswitch sensors incubated with DFHBI and guanine, D-GTP, L-GTP, and adenine in a buffer prepared with DEPC-treated water and RNase-free reagents at 37°C for 30 min. NC, negative control with the natural-chirality or mirror-image riboswitch sensor but without guanine; FU, fluorescence unit. Data are presented as mean ± SD (n = 3) with individual data points. P values were calculated by the Student's two-tailed t test. (**D**) Fluorescence intensities measured at 500 nm of the natural-chirality riboswitch sensor without or with RNase inhibitor and of the mirror-image riboswitch sensor without RNase inhibitor incubated with DFHBI and guanine in a buffer prepared with DEPC-treated water and RNase-free reagents at 37°C for up to 65 days and longitudinally measured at selected time points. NC and MI-NC, negative controls with the natural-chirality or mirror-image riboswitch sensor but without guanine, respectively; FU, fluorescence unit. Data are presented as mean ± SD (n = 3).

the same concentration of guanine, whereas no apparent binding was detected between the natural-chirality and mirror-image riboswitch sensors with D- or L-guanosine triphosphate (GTP) and adenine at the same concentration (Fig. 4C).

When we performed long-term incubation of both the natural-chirality and mirror-image riboswitch sensors under presumed "RNase-free" conditions in a buffer prepared with diethylpyrocarbonate (DEPC)–treated water and RNase-free reagents at 37°C, we observed that the mirror-image riboswitch sensor exhibited a longer estimated half-life than the natural-chirality version without or with RNase inhibitor (Fig. 4D and fig. S63). We validated this result by denaturing PAGE analysis of the natural-chirality and mirror-image riboswitch sensors incubated under the same conditions for up to 65 days, and found that the relative full-length band intensities correlated well with relative fluorescence intensities (fig. S64). We attribute the difference in the stability of the natural-chirality and mirror-image riboswitch sensors to the extraordinary efficiency, stability, and pervasiveness of natural-chirality RNase in the environment (*31*), to which the natural-chirality riboswitch is highly sensitive and the mirror-image riboswitch is resistant.

Stability of kilobase-long L-RNA

We then tested the stability of the unprotected kilobase-long L-RNA in various environments.

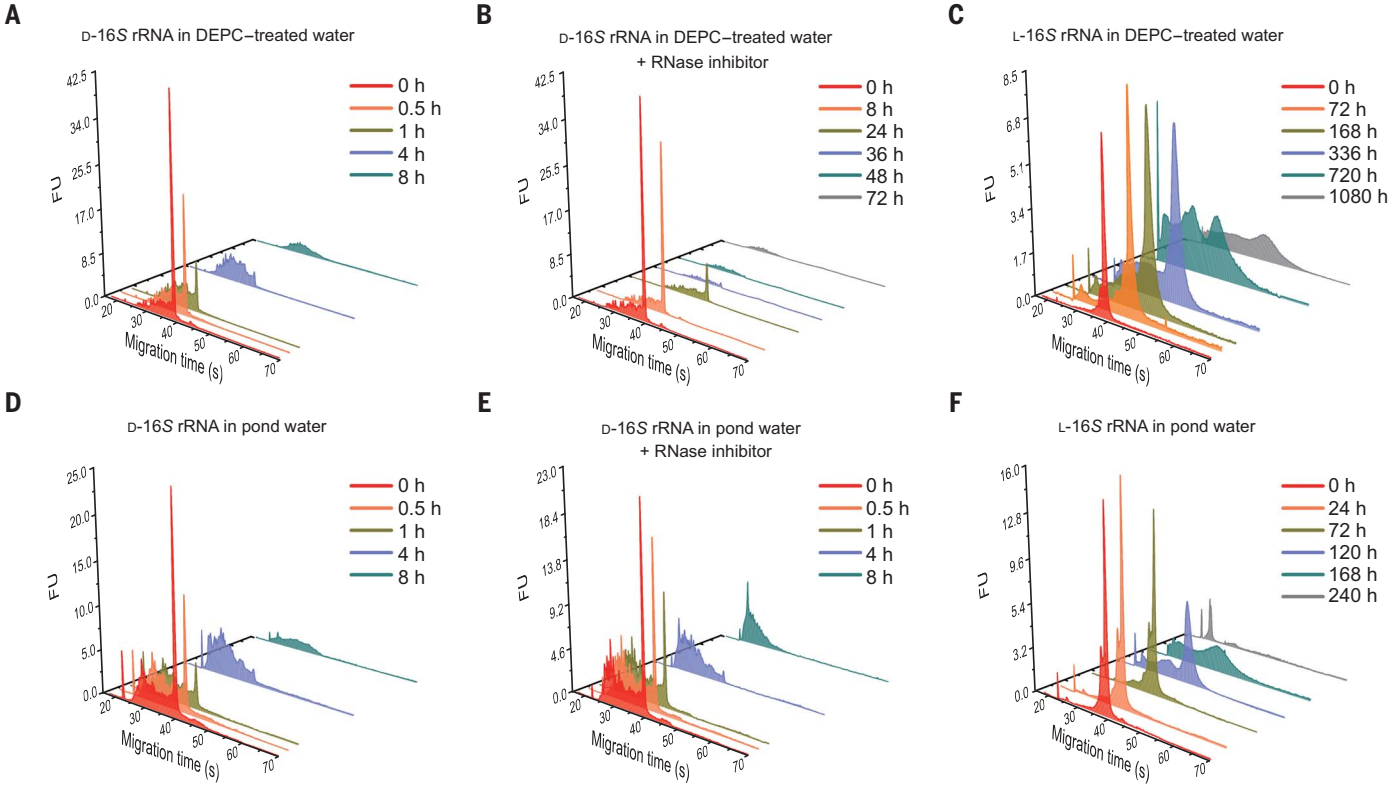

Fig. 5. Stability of kilobase-long L-RNA. (**A** and **B**) Electropherograms of the 1.5-kb natural-chirality 16*S* rRNA incubated in DEPC-treated water at 37°C without (A) or with (B) RNase inhibitor for up to 8 or 72 hours, respectively, and longitudinally measured at selected time points. (**C**) Electropherograms of the 1.5-kb mirror-image 16*S* rRNA incubated in DEPC-treated water at 37°C without RNase inhibitor for up to 1080 hours and longitudinally measured at selected time points. (**D** and **E**) Electropherograms of the 1.5-kb natural-chirality 16*S* rRNA incubated in pond water at 37°C without (D) or with (E) RNase inhibitor for up to 8 hours and longitudinally measured at selected time points. (**F**) Electropherograms of the 1.5-kb mirror-image 16*S* rRNA incubated in pond water at 37°C without RNase inhibitor for up to 240 hours and longitudinally measured at selected time points. FU, fluorescence unit. The corresponding data are also shown in figs. S65 and S67, with the full-length RNA peaks appearing within the migration time of 35 to 45 s.

We incubated the gel-purified natural-chirality and mirror-image 1.5-kb 16*S* rRNAs under presumed RNase-free conditions in DEPC-treated water at 37°C. The natural-chirality 16*S* rRNA, in the absence of RNase inhibitor, was partially degraded after 1 hour and completely degraded after 4 hours (Fig. 5A and figs. S65A and S68). Despite the use of RNase inhibitor, it was partially degraded after 24 hours and completely degraded after 48 hours (Fig. 5B and figs. S65B and S68). By contrast, no substantial degradation of the mirror-image 16*S* rRNA was observed after 72 hours, with partial degradation observed after 336 hours and complete degradation observed after 720 hours (Fig. 5C and figs. S65C and S68).

Next, we incubated the natural-chirality and mirror-image 16*S* rRNAs in pond water at 37°C, and observed that regardless of the use of RNase inhibitor, the natural-chirality 16*S* rRNA was partially degraded after 1 hour and completely degraded after 4 hours (Fig. 5, D and E, and figs. S67, A and B, and S68). By contrast, no substantial degradation of the mirror-image 16*S* rRNA was observed after 72 hours, with partial degradation observed after 120 hours and complete degradation observed after 168 hours (Fig. 5F and figs. S67C and S68). The degradation pattern of the mirror-image 16*S* rRNA in both DEPC-treated water and pond water was different from that of the natural-chirality 16*S* rRNA (Fig. 5 and figs. S65 to S67) in that the full-length L-RNA peak widened before partial and complete degradation took place. This may provide opportunities for future research to reveal the kinetics and underlying mechanisms for the spontaneous hydrolysis of RNA with different lengths and sequences at various pH values, Mg^{2+} concentrations, and temperatures (*32*) without the interference of natural-chirality RNase–catalyzed degradation.

L-Ribozyme–catalyzed L-RNA polymerization

The biostable L-RNA model system may facilitate in vitro studies on ribozymes, particularly for investigating the origins of life, during which most of the modern RNA-processing machinery such as RNase would be presumably absent. Key to the "RNA world" hypothesis is ribozyme-catalyzed RNA polymerization (*33*). The directed evolution of RNA sequences in vitro has revealed various polymerase ribozymes, including the ~180-nt "24-3" and "38-6" polymerase ribozymes, which are capable of amplifying short RNA sequences and polymerizing a 97-nt class I ligase ribozyme, respectively (*34*, *35*). We transcribed the mirror-image 38-6 polymerase ribozyme and single-stranded L-RNA template coding for the class I ligase ribozyme (hereafter referred to as the L-RNA template) by the synthetic mirror-image T7 RNA polymerase (Fig. 6, A to C) with double-stranded L-DNA templates (tables S5 to S7) assembled by mirror-image PCR (*8*). The gel-purified 182-nt L-ribozyme and 112-nt L-RNA template were both resistant to natural-chirality RNase A digestion (Fig. 6, B and C).

We next used the gel-purified mirror-image 38-6 polymerase ribozyme to polymerize the mirror-image class I ligase ribozyme with a 5′-FAM-biotin–labeled L-RNA primer annealed to the gel-purified L-RNA template (Fig. 6A), incubated with L-nucleoside triphosphates (L-NTPs) in 200 mM $MgCl_2$, pH 8.3, at 17°C for up to 10 days. Compared with the D-ribozyme [which exhibited a polymerization efficiency similar to that reported in previous studies (*35*)], the L-ribozyme was almost equally efficient in extending the L-RNA primer to the full length (Fig. 6D), illustrating the high quality of

the mirror-image T7–transcribed L-RNAs. Moreover, we evaluated the stability of the natural-chirality and mirror-image 38-6 polymerase ribozymes, RNA templates, and RNA primers (figs. S69 to S72), and estimated the half-lives of the natural-chirality and mirror-image 38-6 polymerase ribozymes incubated at various Mg^{2+} concentrations. We found that the L-ribozyme exhibited a longer estimated half-life than the natural-chirality version at 2 mM Mg^{2+} concentration (Fig. 6E and fig. S73). With future efforts to discover polymerase ribozymes with lower Mg^{2+} concentration requirements (*36*–*38*), the mirror-image T7–transcribed biostable L-ribozymes may be incubated and evolved in the laboratory for longer periods of time, potentially outperforming their natural-chirality counterparts.

Discussion

The realization of mirror-image T7 transcription may enable a variety of practical applications of high-quality long L-RNAs in diagnostics and therapeutics (*39*–*43*), information storage, computation, imaging, and basic RNA research. Furthermore, the ensemble of efficient mirror-image DNA polymerase, RNA polymerase, reverse transcriptase, and sequencing tools may lead to the realization of a mirror-image selection scheme for the directed evolution and selection of L-RNA aptamers targeting biologically important molecules as potential clinical and research tools (*44*).

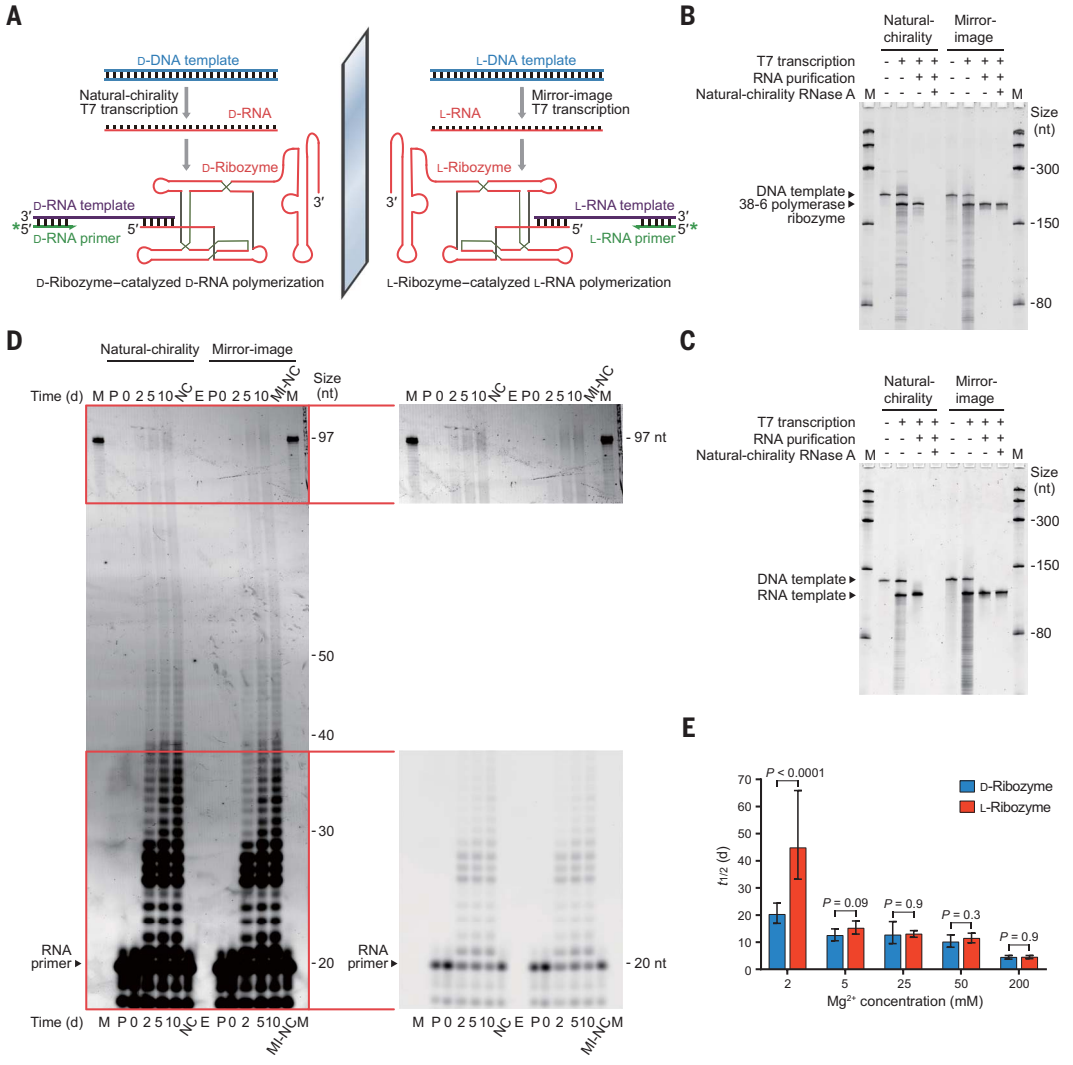

Fig. 6. L-Ribozyme–catalyzed L-RNA polymerization. (**A**) Schematic overview of the natural-chirality and mirror-image ribozyme–catalyzed RNA polymerization using the natural-chirality or mirror-image 38-6 polymerase ribozyme (red) on D- or L-RNA template (purple), prepared by natural-chirality or mirror-image T7 transcription from the double-stranded D- or L-DNA template (blue), respectively, with D- or L-RNA primer (green). (**B** and **C**) Transcription of the natural-chirality and mirror-image 182-nt 38-6 polymerase ribozymes (B) and 112-nt RNA templates (C) from the double-stranded D- or L-DNA template by the synthetic natural-chirality and synthetic mirror-image T7 RNA polymerases, respectively, purified by denaturing PAGE, treated by natural-chirality RNase A, analyzed by denaturing PAGE, and stained by SYBR green II. M, Low Range ssRNA ladder. (**D**) Natural-chirality and mirror-image ribozyme–catalyzed RNA polymerization of the 97-nt class I ligase ribozyme with the natural-chirality or mirror-image 38-6 polymerase ribozyme, RNA template, and 5′-FAM-biotin–labeled D- or L-RNA primer incubated with D- or L-NTPs in 200 mM $MgCl_2$, pH 8.3, at 17°C for up to 10 days and analyzed by denaturing PAGE. Contrast-adjusted images are shown on the right to more clearly show the RNA primers and full-length polymerization products, respectively. NC and MI-NC, negative controls without natural-chirality or mirror-image 38-6 polymerase ribozyme, respectively; E, two empty lanes; P, 20-nt 5′-FAM-biotin–labeled D- or L-RNA primer; M, 97-nt 5′-FAM–labeled D-RNA marker. (**E**) Comparison of estimated half-lives ($t_{1/2}$) of the natural-chirality and mirror-image 38-6 polymerase ribozymes at various Mg^{2+} concentrations. Data are presented as best-fit values and 95% confidence intervals, and the corresponding data for curve fitting are also shown in fig. S73. *P* values were calculated by the extra sum-of-squares *F* test.

Traditional laboratory studies of RNA have been hindered by its rapid degradation resulting from spontaneous hydrolysis and predominantly natural-chirality RNase–catalyzed degradation (*31*), with longer RNAs typically being more vulnerable (Fig. 5 and figs. S65 to S68). Without the interference of natural-chirality RNase–catalyzed degradation, which is virtually unavoidable in laboratory experiments, L-RNAs may serve as an alternative model system for studying RNA spontaneous hydrolysis (*32*). Furthermore, because mirror-image biomolecules behave in a reciprocal manner to their natural-chirality twins, the biostable L-RNA model system may also be applied to a variety of biochemical and biophysical studies in basic RNA research.

To build a mirror-image ribosome that translates D-proteins requires mirror-image rRNAs, tRNAs, mRNAs, r-proteins, and translation factors, the synthesis and in vitro assembly of which can be tested and optimized in the natural-chirality version first, after which the mirror-image version can be synthesized and assembled following the same methodology. Because the mirror-image T7–transcribed L-RNAs contain no RNA modification, the translationally essential modifications of the 16*S* and 23*S* rRNAs (the 5*S* rRNA is known to contain no modifications) (*45*, *46*) can also be validated in the natural-chirality version and may be added either chemically or enzymatically (*11*) to the mirror-image T7–transcribed L-RNAs. Moreover, although the efficiency and fidelity of the synthetic mirror-image T7 RNA polymerase appear sufficient for transcribing the mirror-image rRNAs, tRNAs, and mRNAs for mirror-image translation, the accuracy of mirror-image gene assembly remains to be further improved for preparing high-quality long mirror-image genes (*8*). The realization of mirror-image translation will complete the mirror-image central dogma of molecular biology (Fig. 1A), translating D-proteins and enabling various practical applications such as the directed evolution and selection of biostable D-peptide drugs with a mirror-image version of ribosome or mRNA display (*47*, *48*).

REFERENCES AND NOTES

1. L. Pasteur, *Researches on the Molecular Asymmetry of Natural Organic Products (1860). Alembic Club Reprint No. 14: Edinburgh* (1905).
2. Z. Wang, W. Xu, L. Liu, T. F. Zhu, *Nat. Chem.* **8**, 698–704 (2016).
3. M. Peplow, *ACS Cent. Sci.* **4**, 783–784 (2018).
4. W. Xu *et al.*, *Cell Discov.* **3**, 17008 (2017).
5. W. Jiang *et al.*, *Cell Discov.* **3**, 17037 (2017).
6. A. Pech *et al.*, *Nucleic Acids Res.* **45**, 3997–4005 (2017).
7. M. Wang *et al.*, *Chem* **5**, 848–857 (2019).
8. C. Fan, Q. Deng, T. F. Zhu, *Nat. Biotechnol.* **39**, 1548–1555 (2021).
9. J.-J. Ling *et al.*, *Angew. Chem. Int. Ed.* **59**, 3724–3731 (2020).
10. J. Chen, M. Chen, T. F. Zhu, *Chem* **7**, 786–798 (2021).
11. Y. Liu *et al.*, *Nature* **522**, 368–372 (2015).
12. J. T. Sczepanski, G. F. Joyce, *Nature* **515**, 440–442 (2014).
13. G. A. L. Bare, G. F. Joyce, *J. Am. Chem. Soc.* **143**, 19160–19166 (2021).
14. R. Sousa, S. Mukherjee, *Prog. Nucleic Acid Res. Mol. Biol.* **73**, 1–41 (2003).
15. R. B. Merrifield, *J. Am. Chem. Soc.* **85**, 2149–2154 (1963).
16. P. E. Dawson, T. W. Muir, I. Clark-Lewis, S. B. Kent, *Science* **266**, 776–779 (1994).
17. R. C. Milton, S. C. Milton, S. B. Kent, *Science* **256**, 1445–1448 (1992).
18. L. E. Zawadzke, J. M. Berg, *J. Am. Chem. Soc.* **114**, 4002–4003 (1992).
19. M. T. Weinstock, M. T. Jacobsen, M. S. Kay, *Proc. Natl. Acad. Sci. U.S.A.* **111**, 11679–11684 (2014).
20. A. A. Vinogradov, E. D. Evans, B. L. Pentelute, *Chem. Sci.* **6**, 2997–3002 (2015).
21. J. Weidmann, M. Schnölzer, P. E. Dawson, J. D. Hoheisel, *Cell Chem. Biol.* **26**, 645–651.e3 (2019).
22. R. A. Ikeda, C. C. Richardson, *J. Biol. Chem.* **262**, 3790–3799 (1987).
23. T. H. Segall-Shapiro, A. J. Meyer, A. D. Ellington, E. D. Sontag, C. A. Voigt, *Mol. Syst. Biol.* **10**, 742 (2014).
24. G.-M. Fang *et al.*, *Angew. Chem. Int. Ed.* **50**, 7645–7649 (2011).
25. Q. Wan, S. J. Danishefsky, *Angew. Chem. Int. Ed.* **46**, 9248–9252 (2007).
26. L. Z. Yan, P. E. Dawson, *J. Am. Chem. Soc.* **123**, 526–533 (2001).
27. J. Huang, L. G. Brieba, R. Sousa, *Biochemistry* **39**, 11571–11580 (2000).
28. H. Murakami, A. Ohta, H. Ashigai, H. Suga, *Nat. Methods* **3**, 357–359 (2006).
29. J. S. Paige, T. Nguyen-Duc, W. Song, S. R. Jaffrey, *Science* **335**, 1194 (2012).
30. J. S. Paige, K. Y. Wu, S. R. Jaffrey, *Science* **333**, 642–646 (2011).
31. M. R. Green, J. Sambrook, *Cold Spring Harb. Protoc.* **2019**, pdb.top101857 (2019).
32. Y. Li, R. R. Breaker, *J. Am. Chem. Soc.* **121**, 5364–5372 (1999).
33. G. F. Joyce, J. W. Szostak, *Cold Spring Harb. Perspect. Biol.* **10**, a034801 (2018).
34. D. P. Horning, G. F. Joyce, *Proc. Natl. Acad. Sci. U.S.A.* **113**, 9786–9791 (2016).
35. K. F. Tjhung, M. N. Shokhirev, D. P. Horning, G. F. Joyce, *Proc. Natl. Acad. Sci. U.S.A.* **117**, 2906–2913 (2020).
36. J. Attwater, A. Wochner, P. Holliger, *Nat. Chem.* **5**, 1011–1018 (2013).
37. F. Wachowius, P. Holliger, *ChemSystemsChem* **1**, 1–4 (2019).
38. X. Portillo, Y. T. Huang, R. R. Breaker, D. P. Horning, G. F. Joyce, *eLife* **10**, e71557 (2021).
39. J. T. Sczepanski, G. F. Joyce, *J. Am. Chem. Soc.* **135**, 13290–13293 (2013).
40. J. T. Sczepanski, G. F. Joyce, *J. Am. Chem. Soc.* **137**, 16032–16037 (2015).
41. L. Yatime *et al.*, *Nat. Commun.* **6**, 6481 (2015).
42. D. Oberthür *et al.*, *Nat. Commun.* **6**, 6923 (2015).
43. D. Ji, K. Lyu, H. Zhao, C. K. Kwok, *Nucleic Acids Res.* **49**, 7280–7291 (2021).
44. J. Chen, M. Chen, T. F. Zhu, *Nat. Biotechnol.* (2022).
45. R. Guymon, S. C. Pomerantz, P. F. Crain, J. A. McCloskey, *Biochemistry* **45**, 4888–4899 (2006).
46. J. Mengel-Jørgensen *et al.*, *J. Biol. Chem.* **281**, 22108–22117 (2006).
47. L. C. Mattheakis, R. R. Bhatt, W. J. Dower, *Proc. Natl. Acad. Sci. U.S.A.* **91**, 9022–9026 (1994).
48. R. W. Roberts, J. W. Szostak, *Proc. Natl. Acad. Sci. U.S.A.* **94**, 12297–12302 (1997).

ACKNOWLEDGMENTS

We thank J. Chen, M. Chen, Q. Deng, C. Fan, G. Wang, J. Xu, G. Zhang, and R. Zhao for assistance with the experiments. **Funding:** The work was supported by the National Natural Science Foundation of China (grants 21925702 and 32050178), the Research Center for Industries of the Future (RCIF) at Westlake University, the Westlake Education Foundation, the Tencent Foundation, the Tsinghua-Peking Center for Life Sciences (CLS), and the Beijing Frontier Research Center for Biological Structure. **Author contributions:** Y.X. performed the experiments. Both authors analyzed and discussed the results. T.F.Z. designed and supervised the study and wrote the paper. **Competing interests:** A patent application has been filed relating to this work. The authors declare no other competing interests. **Data and materials availability:** All data are available in the main text or the supplementary materials.

SUPPLEMENTARY MATERIALS

science.org/doi/10.1126/science.abm0646
Materials and Methods
Figs. S1 to S73
Tables S1 to S7
References (*49*–*57*)
MDAR Reproducibility Checklist

View/request a protocol for this paper from *Bio-protocol*.

Submitted 23 August 2021; resubmitted 22 March 2022
Accepted 28 September 2022
10.1126/science.abm0646

Mirror-image T7 transcription of chirally inverted ribosomal and functional RNAs

Yuan XuTing F. Zhu

Science, 378 (6618), • DOI: 10.1126/science.abm0646

Writing genes in mirror image

Large mirror-image enzymes and RNAs are necessary to build mirror-image biology and related applications, but the synthesis of these components has remained challenging. Xu and Zhu chemically synthesized a 100-kilodalton mirror-image T7 RNA polymerase, which enabled efficient and faithful transcription of high-quality l-RNAs as long as 2.9 kilobases. The realization of mirror-image T7 transcription is an important step in synthesizing the mirror-image ribosome toward creating functional in vitro mirror-image biomolecular systems and may provide new opportunities for practical applications in diagnostics and therapeutics. —DJ